Available online at www.sciencedirect.com

SciVerse ScienceDirect

Ceramics International 39 (2013) 6673–6680

CERAMICS INTERNATIONAL

www.elsevier.com/locate/ceramint

Grain growth and crystallinity of ultrafine barium titanate particles prepared by various routes

C.Y. Su[a], Y. Otsuka[a], C.Y. Huang[b], D.F. Hennings[a], C. Pithan[a,*], F.T. Shiao[c], R. Waser[a,d]

[a]*Peter Grünberg Institut, PGI-7: Elektronische Materialien, Forschungszentrum Jülich GmbH, D-52425 Jülich, Germany*
[b]*Ceramics Research Laboratory, Department of Resources Engineering, National Cheng Kung University, No. 1 University Road, Tainan 70101, Taiwan, ROC*
[c]*Walsin Technology Corporation, Kaohsiung, Taiwan, ROC*
[d]*Institut für Werkstoffe der Elektrotechnik II, RWTH Aachen, D-52056 Aachen, Germany*

Received 18 December 2012; received in revised form 25 January 2013; accepted 29 January 2013
Available online 8 February 2013

Abstract

Variations in tetragonal distortion and the degree of crystallinity of ultrafine $BaTiO_3$ particles—both industrially applied criteria qualifying their polar characteristics—upon growth during annealing were studied on powders, prepared by the hydrothermal synthesis and by the oxalate route respectively. Regardless of the synthetic route both these properties were found to develop approximately to the same extent with increasing primary particle size. The degree of crystallinity was detectable only above a critical value of $c/a=1.007$ at an average particle size of around 120 nm. Intragranular porosity in hydrothermal powders and the stoichiometric Ba/Ti-ratio are of minor influence. However, distinct differences in particle growth behavior for both powders were observed. This discrepancy is ascribed to a special morphology of the hydrothermal product, where enhanced particle growth was found to be governed by oriented attachment of individual crystallites and by the motion of solid–solid interfaces.

Keywords: Barium titanate; Nano-powders; Hydrothermal synthesis; Oxalate-route; Oriented attachment

1. Introduction

The permanent trend of miniaturizing electronic components demands for multilayer ceramic capacitors (MLCC) with thin dielectric layers of less than 1 μm in thickness. Dielectric powders with ultrafine particle sizes in the range of 100–200 nm or even less are therefore required for the production of thin layered MLCCs. Various preparation routes have been developed and described [1] for fine-grained $BaTiO_3$ powders, which are nowadays widely industrially employed. Depending on their preparation route, $BaTiO_3$ powders exhibit various morphologies, crystallographic characteristics and quite distinct differences in their coarsening behavior.

An important attribute of $BaTiO_3$ powders, determining the dielectric performance of especially temperature-stable MLCCs, is the degree of the tetragonal distortion of the perovskite unit cell. The tetragonal distortion of the perovskite unit cell of ferroelectric $BaTiO_3$ is characterized by the ratio of the two lattice parameters a and c, corresponding to the lattice planes (200) and (002). Coarse-grained ferroelectric $BaTiO_3$ typically shows a tetragonal distortion of up to $c/a=1.011$ compared to the paraelectric cubic polymorph for which $c/a=1.000$, while fine-grained $BaTiO_3$ often exhibits a pseudo-cubic structure [2]. In the case of temperature stable dielectrics, showing a core–shell structure, the degree of the tetragonal distortion has often been taken as a decisive measure for the permittivity of the grain core phase. A commonly applied industrial criterion for the quality assessment of $BaTiO_3$ powders is the term “crystallinity”. The definition of this arbitrary term is given in Fig. 1. The expression crystallinity involves the peak heights and the splitting of the ideal cubic (200) XRD reflection into two tetragonal (200) and (002) reflections, thus also considering their diffuseness. A crystallinity value C of 50% corresponds to a perfect tetragonal

---

[*] Corresponding author. Tel.: +49 2461615016; fax: +49 2461612550.
E-mail address: c.pithan@fz-juelich.de (C. Pithan).

0272-8842/$ - see front matter © 2013 Elsevier Ltd and Techna Group S.r.l. All rights reserved.
http://dx.doi.org/10.1016/j.ceramint.2013.01.105

lattice. The permittivity of $BaTiO_3$-based dielectric ceramics is determined by the tetragonality ratio c/a and depends on the diffuseness of the XRD reflections (200) and (002). Both parameters are combined in the term "crystallinity", as defined in Fig. 1. The crystallinity of $BaTiO_3$ is a critical measure for the suitability of commercial powders of this compound used for manufacturing of temperature-stable MLCCs with high capacitance. The term crystallinity is therefore commonly employed by MLCC manufacturers for the assessment of industrial $BaTiO_3$ raw materials. In contrast to the tetragonal splitting, c/a which merely represents an averaged crystallographic property of a multitude of individual unit cells, crystallinity also takes into account the effect of the volume fraction of the distorted polar phase.

Tetragonality is reported to be affected by the grain size [3], internal stresses [4] and to some extent also by the stoichiometry ratio Ba/Ti [5] of the $BaTiO_3$ particles. Particle size and morphology of $BaTiO_3$ powders are largely conditioned by the preparation route employed. The crystallinity of $BaTiO_3$ powders, synthesized by different routes, is often rather different: even for a similar primary size and a comparable Ba/Ti-ratio various values of crystallinity are observed. Therefore the changes of crystallinity for $BaTiO_3$ powders as the result of a foregoing thermal treatment have been systematically studied in the presently reported work. Two examples of commercial products, respectively, prepared either by the oxalate route [1] or through hydrothermal synthesis [6], have been considered in detail. Some basic characteristics of these powders are shown in Table 1. Both powders exhibit rather similar properties in the "as-prepared" condition regarding the average particle size d_{50} (determined by laser diffraction), the specific surface area (determined by N_2-absorption), and tetragonality (c/a-ratio determined by Rietveld analysis of the corresponding XRD-diffraction patterns).

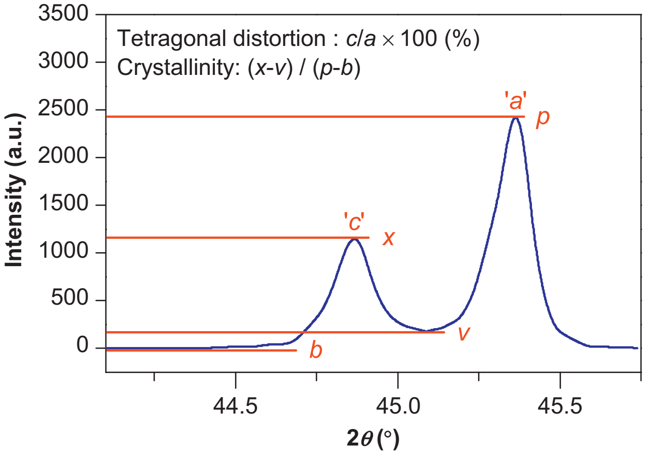

Fig. 1. Derivation of crystallinity of $BaTiO_3$ from (200) and (002) XRD reflections.

Surprisingly, however, on annealing they reveal a quite different development of particle size, tetragonality and crystallinity with temperature. The Ba/Ti-ratio and powder morphology are known to have a strong impact on grain growth. In the case of hydrothermal $BaTiO_3$ also intragranular porosity (Fig. 2) is expected to have a strong effect on the growth behavior and on crystallinity. It is important to note that many of the hydrothermal $BaTiO_3$ particles exhibit a particular crystal habitus showing an approximately cubic shape with flat surfaces.

2. Experimental

For the investigation of crystallinity industrially synthesized hydrothermal $BaTiO_3$ (GC-BT-01Q, Sinocera Functional Material, China) as well as $BaTiO_3$ powder prepared from BaTi-oxalate (HPBT-01A, ZhongXing Electronic Material, China) have been used. Their Ba/Ti-ratio was determined by means of X-ray fluorescence analysis XRF (S8 Tiger, Bruker). For this purpose powder samples are mixed with $Li_2B_4O_7$ (pure grade, AccuSPEC) as fusion flux in the ratio 1:10 by weight and molten at 1100 °C to a homogeneous glass in a Pt crucible. Small discs of frozen glass are then analyzed in the XRF-spectrometer. The impact of the Ba/Ti-ratio on particle growth was studied on $BaTiO_3$ reference powders that were prepared by the conventional Mixed-Oxide (MO) method [1]. These powders were reacted from reagent grade $BaCO_3$ and TiO_2, which were blended in various stoichiometric ratios Ba/Ti ranging from 0.97 to 1.02, thoroughly mixed and thereafter fired for 4 h at 1200 °C in air. The effect of liquid phase enhanced particle growth [7] could be generally excluded in these powders, due to firing temperatures far below the eutectic equilibrium temperature of the solid phases $BaTiO_3$ and $Ba_6Ti_4O_{17}$ at 1320 °C [8], above which at least partial melting occurs.

Hydrothermal and oxalate-based $BaTiO_3$ powders were stepwise heated from 600 °C to 1100 °C for 1 h in air and the evolution of the primary particle size and the resulting morphologies was studied with scanning (SEM) and transmission (TEM) electron microscopy. The evaluation of the

Table 1
Stoichiometry (Ba/Ti-ratio, accuracy: ±0.0005), average particle size (d_{50}), specific surface area (S, accuracy: $\pm 0.01\ m^2/g$) and tetragonality (c/a-ratio) determined by Rietveld refinements for the $BaTiO_3$ powders of the present study. The values for d_{10} and d_{90} are also included. The accuracy in determining these values and the average particle size d_{50} is ±0.005 μm.

Powder	Ba/Ti-ratio	d_{10} (μm)	d_{50} (μm)	d_{90} (μm)	S (m^2/g)	c/a-ratio	Global crystal structure
Oxalate	0.991	0.19	0.42	0.93	9.29	1.0057	Pseudocubic
Hydrothermal	0.998	0.18	0.47	6.07	8.59	1.0053	Pseudocubic

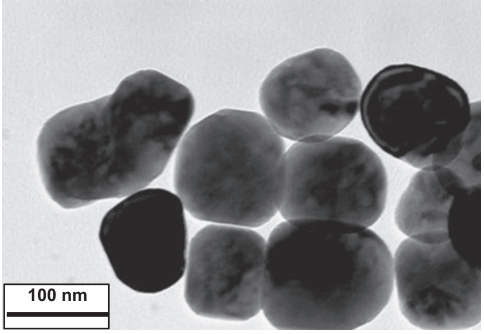

Fig. 2. Hydrothermal $BaTiO_3$ powder—as received— showing intragranular pores in the interior of the particles.

primary particle size using SEM was carried out by measuring the average particle diameter of several hundreds of particles in order to achieve a sufficient statistics. The specific surface area values, S (m^2/g), of the powders were determined by means of N_2-absorbtion (BET-method, Gemini 2360, Micromeritics). The approximate particle size d was determined from the respective S-values using the equation $d=6/\rho S$ (density of $BaTiO_3$: $\rho=6.02$ g/cm^3). The average particle size of powders d_{50} was also measured by the use of a laser diffraction particle size analyzer (Mastersizer Microplus, Malvern). For this purpose a small portion of powder (typically several milligrams) is dispersed in a solution of $Na_4P_2O_7 \cdot 10H_20$ in deionized water. Additionally the primary particle size d was evaluated from SEM powder micrographs and from the broadening of XRD reflections (FWHM: full width at half maximum), using the Scherrer formula [9]. The number N of sub-particles per aggregate was then estimated, using the equation $N=(d_{50}/d)^3$. The particular morphology of hydrothermal $BaTiO_3$ was explored with high-resolution TEM (HR-TEM). All specimens observed by TEM or HR-TEM were first dispersed in ethanol and then deposited on carbon coated Cu-grids, that served as a support for the powder particles. Before the electron microscopic inspection the ethanol was evaporated. The instruments used were a CM-200 TEM (Koninklijke Philips Electronics N.V.) and a 4000 EX HRTEM (JEOL Ltd.).

The tetragonal ratio c/a was evaluated from XRD reflections obtained in reflection (Cu-K$_\alpha$ radiation, Philips X-Pert, Bragg-Brentano geometry) or in high resolution transition mode, and analyzed by the Rietveld method. The corresponding values of crystallinity C were obtained by evaluating the XRD-diffraction patterns according to Fig. 1.

3. Results and discussion

The Ba/Ti-ratio normally has a significant impact on the growth behavior of $BaTiO_3$ powders, as can be seen on the development of the particle size d, evaluated from the SEM micrographs of MO-powders tempered for 4 h at 1200 °C in air, Fig. 3. $BaTiO_3$ exhibits slight solubilities for BaO as well as for TiO_2, adding up to a homogeneity region with respect to the Ba/Ti ratio ranging from 0.983 to 1.005 ($\pm$0.001) at 1200 °C in ambient atmosphere, as reported by Lee et al. [10]. Remarkable changes of the particle size only occur for alterations of the Ba/Ti-ratio within the limits of this homogeneity range. Beyond its limits secondary phases [8] such as Ba_2TiO_4 at Ba/Ti-ratios above 1.025 on the Ba-rich side, and $BaTi_2O_5$ at Ba/Ti-ratios below 0.975 on the Ti-rich side usually occur.

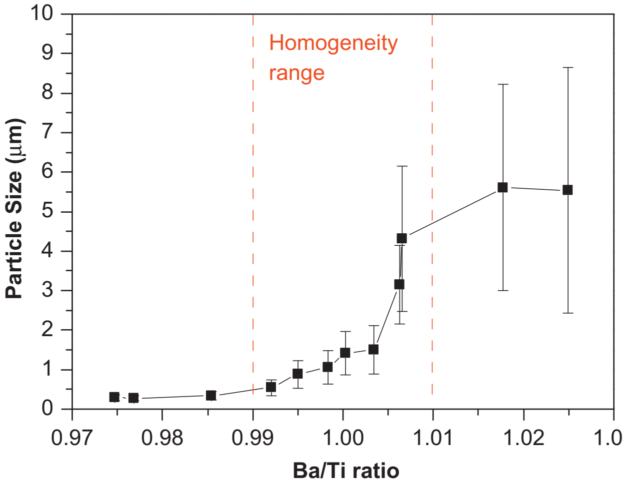

Fig. 3. SEM derived particle size of $BaTiO_3$ prepared through the Mixed Oxide route as a function of the Ba/Ti-ratio. The calcinations were carried out at 1200 °C for 4 h in air.

3.1. *Influence of the Ba/Ti-ratio*

The strong alteration of crystal growth within the homogeneity range of $BaTiO_3$ can be explained by a supposed change of the defect structure, providing Ba-vacancies (V_{Ba}'') for compositions with Ti-excess and Ti-vacancies (V_{Ti}'''') for formulations excessive in Ba. The defect chemical changes of $BaTiO_3$ for these two opposite cases are characterized by the following equations expressed in Kröger–Vink notation:

TiO_2-addition to $BaTiO_3$ (Ba/Ti < 1) :

$$TiO_2 + BaTiO_3 \rightarrow Ba_{Ba}^{\times} + V_{Ba}'' + 2Ti_{Ti}^{\times} + 5O_O^{\times} + V_O^{\bullet\bullet}$$

BaO-addition to $BaTiO_3$ (Ba/Ti > 1) :

$$BaO + BaTiO_3 \rightarrow 2Ba_{Ba}^{\times} + Ti_{Ti}^{\times} + V_{Ti}'''' + 4O_O^{\times} + 2V_O^{\bullet\bullet}$$

The activation energies E for the diffusion of Ba-, Ti- and O-vacancies, as reported by Lewis and Catlow [11], are quite different

$$E(V_{Ti}'''') = 15.12 \text{ eV}; \; E(V_{Ba}'') = 3.45 \text{ eV}; \; E(V_O^{\bullet\bullet}) = 0.62 \text{ eV}.$$

Corresponding to these activation energies the diffusion rate of Ti-vacancies is assumed to be much smaller than that for Ba-vacancies. The low bulk mobility of Ti is therefore considered as rate determining also for the material transport at grain boundaries. With increasing BaO-excess the number of Ti-vacancies notably rises, so that the rate of crystal growth should considerably increase [12]. The role of the much more mobile oxygen vacancies is considered to be less important. When the solubility limits of BaO and TiO_2 are exceeded, further alterations of the Ba/Ti-ratio do not longer change the Ba- and Ti-defect concentrations, resulting in an only minor impact on crystal growth. It is then possibly impeded only by segregation of Ti- or Ba-rich secondary phases.

3.2. Growth of sub-grains and aggregates

The average particle size d_{50}, analyzed by laser diffraction, reveals remarkable differences between the particle growth of hydrothermal and oxalate derived $BaTiO_3$ powders, Fig. 4. The measured d_{50} values display mainly the size of powder aggregates, which are composed of numerous smaller primary particles. As observed on MO-$BaTiO_3$, hydrothermal and oxalate $BaTiO_3$ powders also exhibit a strong impact of the Ba/Ti-ratio on the particle growth. The excess of 1 mol% TiO_2 in oxalate powder strongly retards the crystal growth, while almost stoichiometric hydrothermal $BaTiO_3$, showing a value of $Ba/Ti \approx 1.000$, exhibits more pronounced crystal growth. The size d_{50} of hydrothermal $BaTiO_3$ particles begins to increase which is already below 600 °C, showing a rapid rise at temperatures above 800 °C. The particle growth of oxalate derived $BaTiO_3$—in contrast—is comparatively small and only starts moderately at temperatures above 800 °C.

Fig. 5 shows the evolution of the primary particle size d with increasing annealing temperature for hydrothermally synthesized and oxalate derived $BaTiO_3$, as evaluated by the Scherrer method and from SEM micrographs. Both methods reveal a similar growth trend, but provide an approximately twice larger particle size in the case of SEM evaluation compared to XRD. This observed difference is probably due to a systematic error of the Scherrer method, which is principally only valid for particles smaller than 100 nm. Particle sizes derived from the specific surface area S were substantially larger than those determined by SEM and the Scherrer method. The large particle sizes derived from S are probably due to strong particle conglomeration and sintering, Fig. 6. Consequently, the values evaluated from SEM micrographs were regarded as the most reliable ones, at least for higher annealing temperatures.

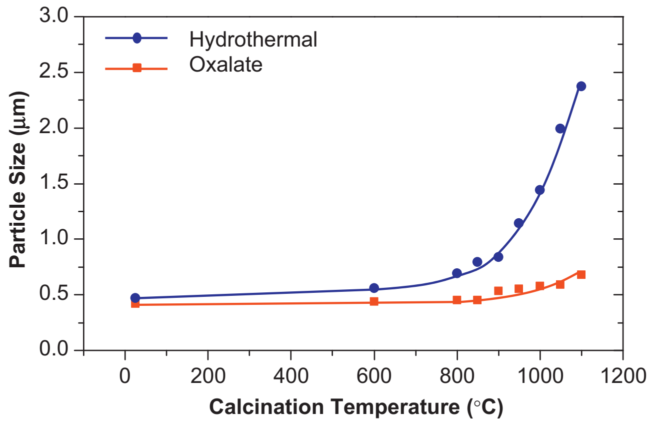

Fig. 4. Increase of the average particle size, d_{50}, of hydrothermally prepared and oxalate derived $BaTiO_3$ powder annealed at different temperatures in ambient atmosphere. The accuracy in determining the particle size is ±0.005 µm.

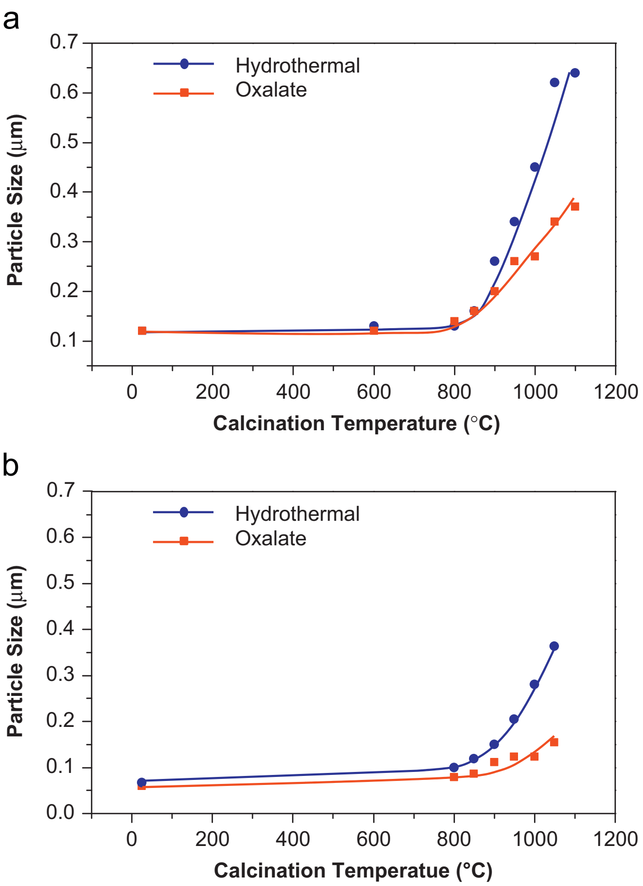

Fig. 5. Sub-particle size d of annealed hydrothermally prepared and oxalate derived $BaTiO_3$, evaluated from SEM (a) and XRD (b). The standard error in determining the particle size by SEM was different for every calcination temperature and varied between 4 nm and 26 nm. The accuracy of the data shown in (a) can therefore be specified by ±0.005 µm. The size error estimated from XRD is ±0.002 µm.

The number N of sub-particles per aggregate develops quite dissimilar with increasing annealing temperature for both powders, Fig. 7. For the oxalate derived powder a continuous decline of the number of sub-particles per aggregate is observed for temperatures above 600 °C. On the other hand a distinct increase in N with rising annealing temperatures above 600 °C is observed in the case of hydrothermally grown powders, yielding a maximum value of approximately around 150 at 800 °C. For higher temperatures a lower, almost constant value of only 40 sub-particles per agglomerate is obtained. This strong enhancement of N for hydrothermal $BaTiO_3$ at temperatures between 600 °C and 900 °C cannot be simply explained in terms of the Ba/Ti-ratio but is most probably due to an individual and specific particularity in powder morphology. The increase of N in the intermediate temperature range indicates a pronounced coarsening of aggregates in the hydrothermal powder. At 800 °C many of the originally

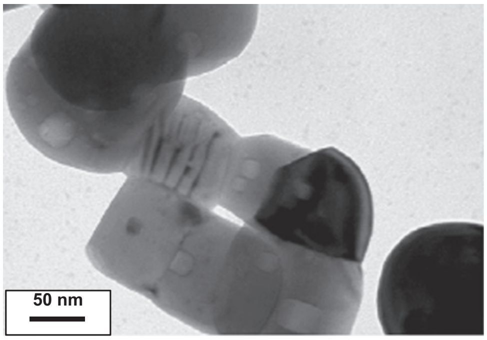

Fig. 6. TEM micrograph showing hydrothermally prepared $BaTiO_3$ particles that were conglomerated via "attached growth" during annealing at 800 °C. Initially spherical internal pores become cubic shaped. The edges of these pores are almost parallel to the edges of the crystallites they are contained in and also parallel from one particle to a neighboring one suggesting crystallographic texturing during annealing.

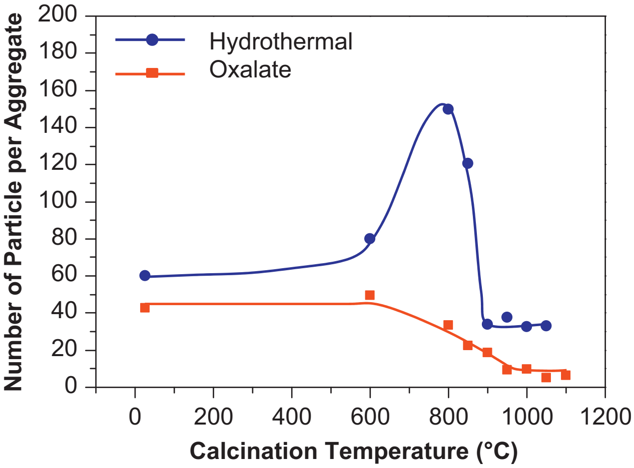

Fig. 7. Number of sub-particles per aggregate of hydrothermal prepared and oxalate derived $BaTiO_3$ annealed at different temperatures.

spherical hydrothermal particles became cube-shaped and were conglomerated via attachment of parallel edges, Fig. 6. Already Shi et al. [13] demonstrated and evidenced by the use of HR-TEM a material transport along the grain surfaces of hydrothermally grown $BaTiO_3$ particles. The sharp decline of the particle number N at more elevated temperatures above 900 °C, on the other hand, is most probably the result of coalescent sub-particles in these aggregates, caused by an Ostwald-type ripening process, Fig. 7.

In order to elucidate this phenomenon in more detail, the crystallographic orientation of hydrothermally synthesized and oxalate derived $BaTiO_3$ sub-particles has been evaluated from lattice fringes, Fig. 8. A TEM investigation of the hydrothermal $BaTiO_3$ powders, revealed a particular and distinct morphology, showing numerous nano-sized particles connected to each other in oriented attachment. The major part of the nano-particles, however, was found to be randomly oriented. Oriented attachment has already been reported [14] for hydrothermally grown nano-particles in various material systems. Cube-like monodisperse nanoparticles of $BaTiO_3$ were prepared by a solvothermal route and used for the design of ordered arrays [15]. The rapid merging of particles to large aggregates is probably supported by this mechanism. In the case of fine porous Al_2O_3 aggregates Greskovich [16] described for the initial stage of coarsening the motion of grain boundaries from larger toward smaller particles. While coalescence of oxalate derived $BaTiO_3$ probably occurs mainly via surface diffusion, coarsening of hydrothermal $BaTiO_3$ is also

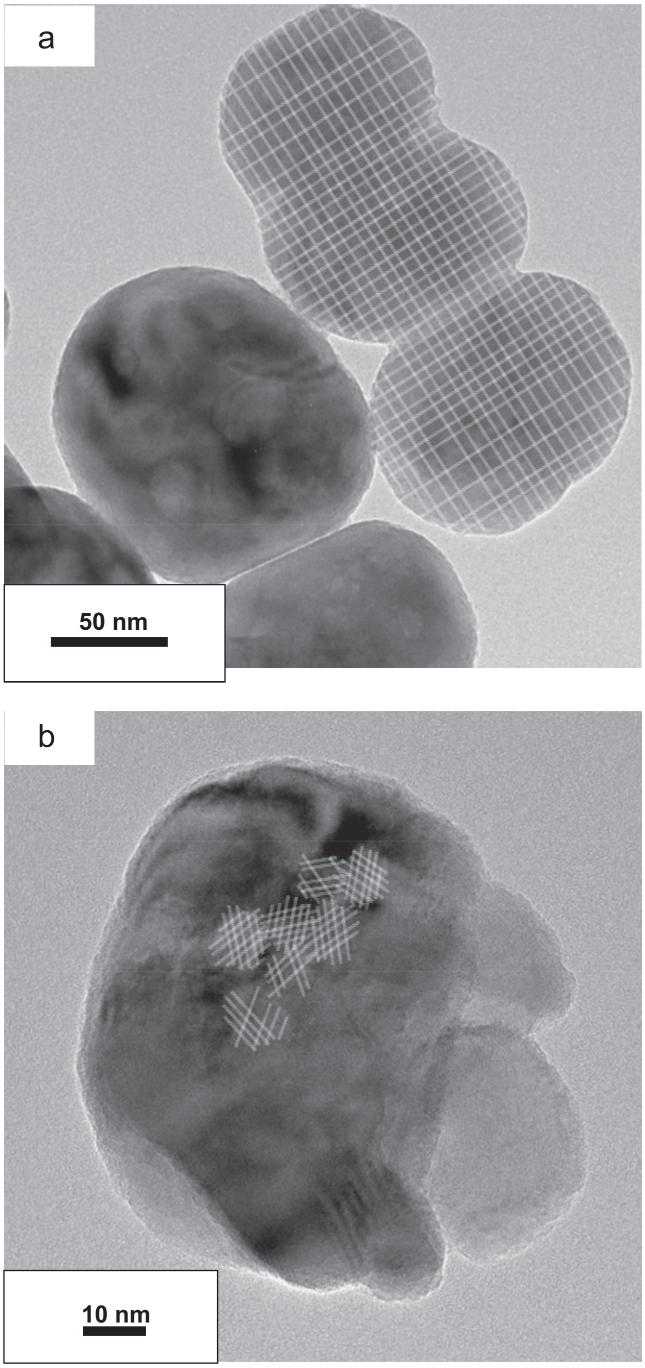

Fig. 8. HRTEM lattice fringes of assembled sub-particles in $BaTiO_3$ powders: (a) hydrothermally prepared and (b) oxalate based powders.

governed by volume diffusion and the motion of solid–solid interfaces.

In contrast to the hydrothermal powders sub-particles of oxalate derived $BaTiO_3$ appeared in random orientation. Oxalate $BaTiO_3$ emerges from thermal decomposition of $BaTi(C_2O_4)_2 \cdot 4H_2O$ at temperatures above 800 °C [1]. Even small particles around 100 nm in diameter are composed of many tiny, randomly oriented sub-crystallites, partly with a size of a few tens of nanometers, Fig. 8. No oriented attachment of the crystallites was observed in those powder aggregates. During heating the tiny crystallites continuously coalesce to larger ones. This sluggish crystal growth is most probably controlled by grain boundary diffusion, which is rather slow according to the excess of TiO_2 in those powders and the comparatively small number of Ti-vacancies.

Hydrothermal $BaTiO_3$ powders annealed at 800 °C show cubically shaped internal pores arising from the conglomeration of vacant lattice sites present on all—anionic as well as cationic—positions, as it is typically observed for hydrothermal particles [1]. The pores obviously possess also a preferred crystallographic orientation to each other within the crystal structure. Since the particles have grown via aligned attachment the edges of these almost quadratic pores are practically parallel to each other not only within one and the same particle but also from one particle to a neighboring one. This observation supports the idea of growth via aligned attachment. HR-TEM observations, exemplarily shown in Fig. 9, confirm the preferred crystallographic orientation relationship of the hydrothermally grown $BaTiO_3$ particles.

3.3. Crystallinity and tetragonality

“As-received” powders of oxalate-based and hydrothermal $BaTiO_3$ both exhibited a primary particle size smaller than 100 nm (evaluated from XRD). Both these powders also revealed an almost pseudocubic crystallographic structure. Simultaneously with the onset of crystal growth, the tetragonal distortion of hydrothermal $BaTiO_3$ also steeply increases during annealing, approaching already the theoretical and maximum possible value of the tetragonality ratio $c/a = 1.011$ at annealing temperatures around 1000 °C. At this stage the average particle size amounts to approximately 200 nm. The tetragonal distortion of the oxalate derived $BaTiO_3$ powder, however, remained almost constant ($c/a \approx 1.0055$) at annealing temperatures below 800 °C and only attained a comparatively much lower value of $c/a = 1.008$ upon tempering at 1100 °C. However, as can be recognized from Fig. 10, the tetragonal distortion c/a of both, hydrothermally grown and oxalate derived powders, is entirely determined by the sub-particle size d. Morphological features, e.g. intra-granular porosity,

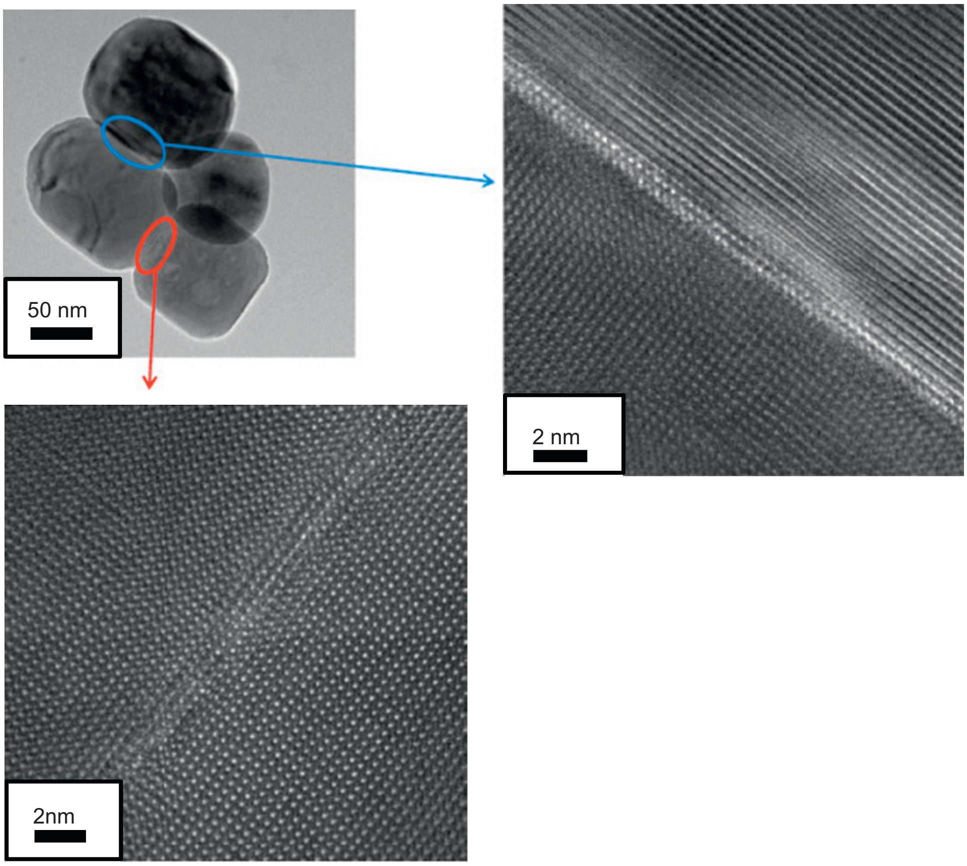

Fig. 9. TEM micrograph of agglomerated $BaTiO_3$ powder particles (as received condition) coarsened by the mechanism of “attached growth” and high resolution TEM showing the crystallographic orientation relation at two different examples of solid–solid interfaces.

oriented attachment and differences in the concentration of lattice defects, according to different Ba/Ti-ratios, obviously have only a negligible effect on the c/a-ratio.

Almost identical values of the sub-particle size, the tetragonal distortion c/a and crystallinity C have been found for hydrothermal and oxalate $BaTiO_3$ annealed at 850 °C and 1000 °C respectively, Table 2. Both powders, annealed at different temperatures were around 120 nm in size, showed almost the same tetragonal distortion $c/a=1.0075$ and nearly indistinguishable values of crystallinity $C=3.8$–3.9%. However, in contrast to the continuous increase of c/a with the sub-particle size d, the crystallinity, which is determined by the diffuseness of overlapping (002) and (200) reflections, began to increase from ca. 4% at $c/a=1.0075$ up to about 40% at $c/a=1.01$ only in the case of hydrothermally prepared powders. Due to the retarded grain growth of the oxalate derived powders such high values of crystallinity could not be achieved on annealing up to 1050 °C.

Fig. 11 shows the relationship between crystallinity C and tetragonality c/a for both cases. It appears that below a critical particle size of 120 nm the crystallinity, corresponding to the volume portion of the tetragonally distorted polymorph of $BaTiO_3$, is negligibly small, although the tetragonality c/a has already achieved 70% of the maximum theoretical value. This behavior is the same in both powder batches: oxalate derived and hydrothermally processed $BaTiO_3$. Independent of the synthetic route applied for the preparation of the powders crystallinity starts to increase almost linearly with tetragonality above a critical value $(c/a)_{\text{crit.}} \approx 1.007$, Fig. 11.

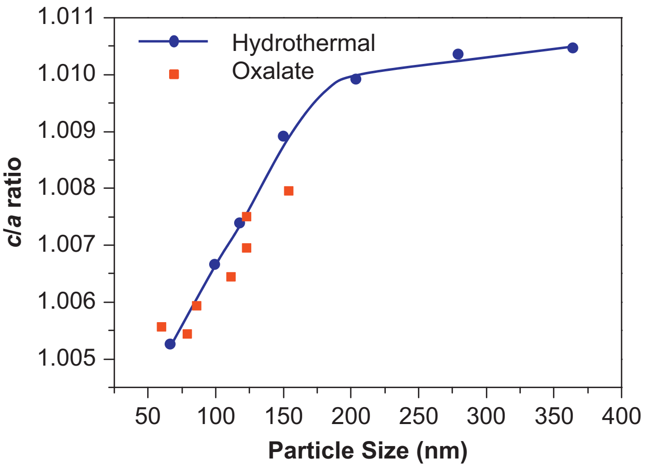

Fig. 10. Dependence of the tetragonality ratio c/a from primary particle size for hydrothermally processed and oxalate derived $BaTiO_3$ powders annealed at various temperatures. The number of significant digits for the lattice parameter is 5.

In scientific literature the tetragonality of $BaTiO_3$, which has for example been extensively summarized in a review by Yoon [17], has often been treated as the most relevant criterion to assess the functionality of ultrafine grained $BaTiO_3$ powders or ceramics. Many reports aimed to determine the critical particle or grain size, below which ferroelectricity is believed to be entirely suppressed due to the stabilization of the pseudocubic polymorph of $BaTiO_3$. In this context, for long, diffraction methods have been applied to investigate the crystallography of $BaTiO_3$ as a function of crystallite size in combination with electrical methods in order to determine the size-effect on the dielectric behavior of this compound [18,19]. These efforts resulted in the preliminary conclusion that very small crystallites of $BaTiO_3$ apparently consist of a tetragonal distorted polar core and a surrounding dead surface layer. Later studies taking advantage of more advanced analytical tools, such as piezoresponse measurements using atomic forces microscopy [20] or Raman-spectroscopy [21,22] also evidenced locally isolated polar clusters in ultrafine $BaTiO_3$-crystallites being only several few tens of nanometers large, that still show a tetragonal distortion and to some extent also ferroelectric activity. From the perspective of industrial application, it should be noted that not only the lattice parameter of tetragonal $BaTiO_3$ but also the volume portion present is a relevant criterion. In this context, the present report shows for two widely applied synthetic routes used in the practice of capacitor manufacturing that crystallinity of $BaTiO_3$ apparently only evolves above a certain critical value of tetragonality, which does not seem to depend on extrinsic effects related to powder preparation.

4. Summary and conclusions

The tetragonal distortion c/a of the perovskite unit cell of $BaTiO_3$ powders, derived by means of XRD was found to be dependent almost entirely on the sub-particle size only. Different preparation routes, e.g. the oxalate method or hydrothermal processing, have negligible influence on c/a. Intra-granular porosity and different Ba/Ti-ratio are also of minor importance. However, even for well measurable ratios

Table 2
Tetragonality (c/a-ratio) and crystallinity of different selected powders in the annealed condition. The accuracy for determining d_{Scherrer} is ± 0.002 µm. The number of significant digits for the lattice parameter is five. This means that the accuracy of c/a is ± 0.00005.

Powder	T_{anneal} (°C)	d_{Scherrer} (µm)	c/a-ratio	Crystallinity (%)
Hydrothermal	850	0.12	1.0074	3.867
Hydrothermal	1050	0.36	1.0100	40.11
Oxalate	1000	0.12	1.0075	3.833
Oxalate	1050	0.15	1.0080	7.733

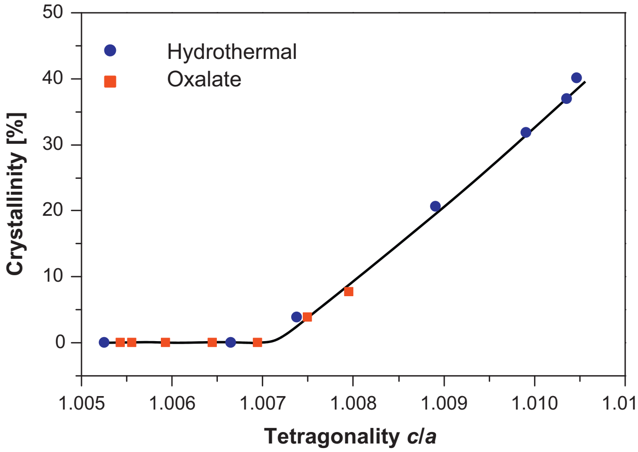

Fig. 11. Relation between the crystallinity and the tetragonality ratio c/a for hydrothermally processed and oxalate derived $BaTiO_3$ powders annealed at various temperatures.

up to $c/a \approx 1.007$ the (002)/(200) reflections feature a pseudocubic complex, showing zero crystallinity. The term crystallinity, considering the diffuseness of the reflections, therefore seems to be more qualified to assess the perfection of the lattice and the quality of the $BaTiO_3$ powder than tetragonality only.

The particle growth behavior of $BaTiO_3$ powders is basically determined by the Ba/Ti ratio. The impact of the Ba/Ti-ratio on the grain growth rate can be explained by different mobilities of Ba- and Ti-vacancies, corresponding to Ba- or Ti-excess respectively. The notable change of the growth rate with the Ba/Ti-ratio of $BaTiO_3$ is limited to the narrow homogeneity range $Ba/Ti \approx 1 \pm 0.01$. Beyond this solubility limit the growth rate remains almost unaffected from changes of the Ba/Ti-ratio. In hydrothermal $BaTiO_3$ a considerable number of sub-particles are arranged in oriented attachment. This special morphology of the hydrothermal $BaTiO_3$ powder allows a rapid coalescence and enlargement of particle aggregates. Increasing formation of cube-like nano-particles, oriented attachment and coalescence to larger aggregates is already observed at temperatures below 800 °C in hydrothermal $BaTiO_3$. Grain boundary movement between attached grains is supposed to speed up the coalescence of sub-particles and aggregates at temperatures below 800 °C. In oxalate powders, showing a random orientation of sub-particles, coalescence takes place within the aggregates at temperatures above 800 °C.

The common criterion "crystallinity" can be successfully applied for the quality assessment of industrial $BaTiO_3$ powders, because it closely relies on the sub-particle size. Even diverse powders like hydrothermal and oxalate $BaTiO_3$ exhibit identical crystallinity, as far as they show comparable sub-particle size. Sub-particle sizes can be easily regulated and adapted by appropriate thermal treatment. However, different thermal treatments are required, if the powders exhibit different rates of crystal growth.

References

[1] C. Pithan, D. Hennings, R. Waser, Progress in the synthesis of nanocrystalline $BaTiO_3$ powders for MLCC, International Journal of Applied Ceramic Technology 2 (1) (2005) 1–14.

[2] G.H. Jonker, W. Noorlander, Grain size of sintered barium titanate, in: G.H. Stewart (Ed.), in: Science of Ceramics I, Academic, London, 1962, pp. 255–264.

[3] G. Arlt, D. Hennings, G. de With, Dielectric properties of fine-grain barium titanate ceramics, Journal of Applied Physics 58 (4) (1985) 1619–1625.

[4] W.R. Buessern, L.E. Cross, A.K. Goswami, Phenomenological theory of high permittivity in fine-grained barium titanate, Journal of the American Ceramic Society 49 (1) (1966) 33–36.

[5] S. Lee, Z.-K. Liu, M.-Ho Kim, C.A. Randall, Influence of non-stoichiometry on ferroelecxtric phase transition in $BaTiO_3$, Journal of Applied Physics 101 (2007) 054119.

[6] D. Hennings, G. Rosenstein, H. Schreinemacher, Hydrothermal preparation of barium titanate from Ba–Ti-acetate gel precursors, Journal of the European Ceramic Society 8 (2) (1991) 107–115.

[7] D.F. Hennings, R. Janssen, P.J.L. Reynen, Control of liquid-phase-enhanced discontinuous grain growth in barium titanate, Journal of the American Ceramic Society 70 (1) (1987) 23–27.

[8] H.M. O'Bryan Jr., J. Thomson Jr., Phase equilibria in the TiO_2-rich region of the system BaO–TiO_2, Journal of the American Ceramic Society 57 (12) (1974) 522–526.

[9] H.P. Klug, L.E. Alexander, X-ray Diffraction Procedures for Polycrystalline and Amorphous Materials, vol. 687, Wiley, New York, 1974.

[10] S. Lee, C.A. Randall, Z.K. Liu, Comprehensive linkage of defect and phase equilibria through ferroelectric transition behavior in $BaTiO_3$-based dielectrics: part 1. Defect energies under ambient air conditions, Journal of the American Ceramic Society 91 (6) (2008) 1748–1752.

[11] G.V. Lewis, C.R.A. Catlow, Computer modeling of barium titanate, Radiation Effects 73 (1-4) (1983) 307–314.

[12] J. Novotny, M. Rekas, Defect structure, electrical properties and transport in barium titanate VII. Chemical diffusion in Nb-doped $BaTiO_3$, Ceramics International 20 (4) (1994) 265–275.

[13] J.L. Shi, Y. Deguchi, Y. Sakabe, Relation between grain growth, densification and surface diffusion in solid state sintering—a direct observation, Journal of Materials Science 40 (21) (2005) 5711–5719.

[14] M.P. Finnegan, H. Zhang, J.F. Banfield, Anatase coarsening kinetics under hydrothermal conditions as a function of pH and temperature, Chemistry of Materials 20 (10) (2008) 3443–3449.

[15] S. Adireddy, C. Lin, B. Cao, W. Zhou, G. Caruntu, Solution-based growth of monodisperse cube-like $BaTiO_3$ colloidal nanocrystals, Chemistry of Materials 22 (6) (2010) 1946–1948.

[16] C. Greskovich, K.W. Lay, Grain growth in very porous Al_2O_3 compacts, Journal of the American Ceramic Society 55 (3) (1972) 142–146.

[17] D.-H. Yoon, Tetragonality of barium titanate powder for ceramic capacitor application, Journal of Ceramic Processing Research 7 (4) (2006) 343–354.

[18] M.H. Frey, D.A. Payne, Grain-size effect on structure and phase transformations for barium titanate, Physical Review B 54 (5) (1996) 3158–3168.

[19] M.H. Frey, Z. Xu, P. Han, D.A. Payne, The role of interfaces on an apparent grain size effect on the dielectric properties for ferroelectric barium titanate ceramics, Ferroelectrics 206 (1) (1998) 337–353.

[20] M.T. Buscaglia, M. Viviani, V. Buscaglia, L. Mitoseriu, A. Testino, P. Nanni, Z. Zhao, M. Nygren, C. Harnagea, D. Piazza, C. Galassi, High dielectric constant and frozen macroscopic polarization in dense nanocrystalline $BaTiO_3$ ceramics, Physical Review B 73 (2006) 064114.

[21] Y. Shiratori, C. Pithan, J. Dornseiffer, R. Waser, Raman scattering studies on nanocrystalline $BaTiO_3$. Part I—isolated particles and aggregates, Journal of Raman Spectroscopy 38 (2007) 1288–1299.

[22] Y. Shiratori, C. Pithan, J. Dornseiffer, R. Waser, Raman scattering studies on nanocrystalline $BaTiO_3$. Part II—consolidated polycrystalline ceramics, Journal of Raman Spectroscopy 38 (2007) 1300–1306.